

Progression and Application of Photocatalytic Membrane Reactor for Dye Removal: An Overview



Ayushman Bhattacharya and Selvaraj Ambika

Abstract Globally, textile industries are one of the rapidly growing industrial sectors that are not only contributing significantly towards the economy but are also generating an extensive variety of dyes as pollutants that vitiates the natural ecosystem. The increasing toxicity and recalcitrant nature of the industrial dye effluents are emerging concerns that require immediate attention. Treatment of dye-enriched water bodies and industrial effluents with advanced, economical, sustainable and efficacious technology is the need of the hour. The heterogeneous photocatalysis, an advanced oxidation process (AOP), is a novel and sustainable process that ensures photocatalytic degradation of dyes by generating reactive and oxidizing free radicals under ultraviolet (UV) and visible irradiation. Besides, integrating the membrane separation process with heterogeneous photocatalysis results in a holistic approach—photocatalytic membrane reactor (PMR). The PMR is reported to aid in (i) achieving higher pollution removal efficiency with complete detoxification and (ii) abating the membrane fouling. Coupling the fact of necessity to treat dye-contaminated water and the effective application of PMR, this chapter aims to elucidate the properties and classification of dyes, photocatalytic reaction mechanism and membrane fabrication methods. Also, the chapter conveys comprehensive information and fundamental understanding of different configurations and applications of Photocatalytic Membrane Reactor (PMR) with major emphasis on recent advancements.

Keywords Photocatalytic Membrane Reactor · Auxochrome · Chromophore · Dye Sensitization · Membrane Fabrication · Photocatalysis · Dye Removal

A. Bhattacharya · S. Ambika (✉)
Department of Civil Engineering, Indian Institute of Technology, Hyderabad, India
e-mail: ambika@ce.iith.ac.in

© The Author(s), under exclusive license to Springer Nature Singapore Pte Ltd. 2022
S. S. Muthu and A. Khadir (eds.), *Membrane Based Methods for Dye Containing Wastewater*, Sustainable Textiles: Production, Processing, Manufacturing & Chemistry, https://doi.org/10.1007/978-981-16-4823-6_4

1 Introduction

Dyes are organic compounds that persist as an environmental pollutant and are mutagenic, carcinogenic and toxic, and can endorse biomagnification [40]. Augmented production, production and utilization of dyes generates a huge amount of dye-contaminated water from industries. Industries mainly responsible for the discharge of dyes are textile industries (54%), dyeing industries (21%), pulp and paper industry (10%), paint and tanning industry (8%), dye concocting industry (7%), revealing textile industry as the major polluter [55]. The incomplete removal of dyes in treatment processes, due to the recalcitrant nature, reinforced their presence in surface water and groundwater and is becoming a matter of great concern worldwide [33]. This further has adversely affected the environment and the health of mankind. Besides, the existence of dyes in the aquatic ecosystem impedes the photosynthetic activity which eventually lowers the dissolved oxygen and thereby posing a threat to aquatic species. Conventional treatment methods for the treatment of organic contaminants are adsorption, biological treatment and coagulation–flocculation-based physiochemical treatment. The coagulation-flocculation has limited application due to the lower decolourization efficiency for the reactive and vat dyes along with higher sludge generation, and operational cost [25]. In the case of adsorption, pollutants are trapped in the high surface area of the adsorbents and exhibit higher colour removal efficiency from wastewater comprising of dyes. Generally, activated carbon is used as an adsorbent as it is cheap, but possess poor reusability and generates secondary waste that needs supplementary treatment. In the case of biological treatment, soluble organic dyes are easily degraded, whereas non-soluble dyes, containing heterocyclic, polyaromatic hydrocarbons (PAHs), and polychlorinated biphenyls (PCBs) in their structure, are resistant to the biological process. In addition, biological processes require large land and suitable operating conditions as the bacterial populations are very sensitive. Hence, there is a need for a robust treatment technique that overcomes the above-said limitations and results in the complete eradication of dyes from aqueous solution.

Advanced oxidation process (AOP) such as heterogeneous photocatalysis involves the usage of semiconductor particles for the generation of highly oxidative radicals under UV–Visible irradiation. This oxidizes and degrades the non-selective organic pollutants and transforming them into mineralized products [60]. Though the precious photocatalyst particles are efficient, due to the huddle in collecting these particles for reuse, the process becomes resource-intensive and costly. This compels attaching the particles to a template without compromising the function. In the arena of wastewater and water treatment, the application of membranes is one of the promising separation techniques which holds the advantages of enhanced eradication of pollutants, tailor made to have a broader range of pollutants removal and energy-efficient. Microfiltration (MF), Nanofiltration (NF), Reverse osmosis (RO) and ultrafiltration (UF) are the generally employed membrane technologies [71]. The challenges associated with the conventional membranes include membrane fouling and the inability to degrade pollutants [70].

To synergize the benefits of photocatalysis and membrane-based treatment techniques, and to overcome the drawbacks, the photocatalyst particles can be attached on the membrane surface which results in photocatalytic membrane reactor (PMR). This PMR fosters photocatalysis of dyes and separation of products in one step with strict adherence to the green chemistry principle. Furthermore, the integration of the processes vanquishes the associated challenges of single treatment units. Having understood the importance of PMR in dye removal from the aqueous medium, this chapter outlines the properties and classification of dyes in use, mechanism of photocatalytic reactions and membrane fabrication methods. Correspondingly, the chapter discusses the different configurations and applications of Photocatalytic Membrane Reactor (PMR) with major emphasis on recent advancements.

2 Dyes Classification

Dyes are the unsaturated organic compounds that contain auxochromes and chromophores. Electronic properties of the chromophore molecules like double or triple bond-containing carbon-carbon, carbon-oxygen, nitrogen-nitrogen and carbon-nitrogen atoms influence the colour imparted by the dyes to the solution and are liable for the absorption of light in the UV visible spectrum that leads to excitation of electrons. The compound appears to be coloured when two conditions are fulfilled (i) chromophore molecules should be linked with a conjugated system, inducing bathochromic shift and (ii) the light absorption should take place in the visible spectrum (400–800 nm) [29]. Therefore, depending upon the structure of the dye molecule and the light absorption in UV visible spectrum, the chromophore molecules will cede the colour to the dyes. Based on the above understanding, Fig. 1a infers that chromophore molecules linked with aromatic ring generate colour, whereas no colour was produced when chromophore molecules were placed between methyl groups as shown in Fig. 1b. Both the wavelength and intensity of absorption vary when the covalent saturated group, i.e. auxochromes (NH_2 , OH , COOH , SO_3 , halogen, etc.) gets bonded with the chromophore [9, 24]. Auxochrome does not produce colour but modifies the light absorbing ability of the chromophore resulting in the colour

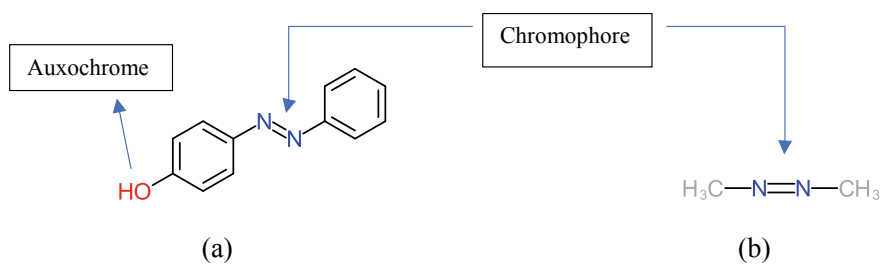


Fig. 1 a 4-Hydroxyazobenzene (Gurses et al. 2016) b Azomethane (Colourless) [29]

intensification of the dye, and therefore, they are known as colour enhancing group [59], (Gurses et al. 2016). Besides, the presence of auxochrome enhances the solubility of the dye and its affinity towards the fibre [55]. In aromatic dye structure, presence of electron donors like hydroxyl, carboxylic and nitrite group assists in electrophilic attack due to increase in electron density on the phenyl ring because of resonance effect causing higher photodegradation rate, whereas presence of chloro group reduces the photodegradation rate and renders the aromatic structure inactive due to their electron withdrawing tendency. Studies have revealed that the presence of any functional group that induces lower solubility of the dye molecules, depresses the rate of photodegradation. That is why higher alkyl chains are responsible for lowering of photodegradation rate [32].

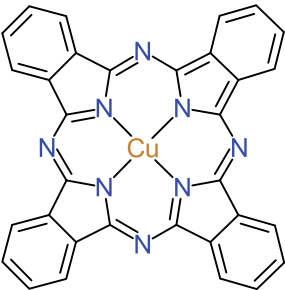
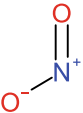
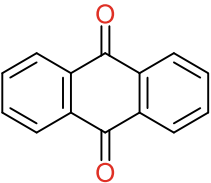
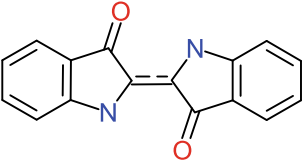
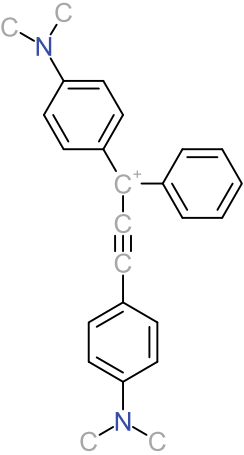
The dyes can be classified based on two features (i) chemical structure, more specifically on the chromophore grouping and (ii) applications [9, 10]. On the basis of chromophore grouping, dyes are categorized as azo dyes, indigo dyes, anthraquinone dyes, phthalocyanine dyes, xanthene dyes, phthalein dyes, nitrated and nitrosated dyes, oxazine, polymethinic dyes, acridine, diphenylmethane and triphenylmethane dyes as shown in Table 1. Among them, azo dyes are commonly employed in industrial applications and are non-biodegradable [13, 67]. Azo dyes comprise of double bond nitrogen atoms ($-N = N -$) and are classified as mono-azo, di-azo, tri-azo and poly azo depending upon the number of ($-N = N -$) bonds in the structure. The Van der Waals force of attraction between fibres and azo dyes gets fortified due to the presence of aromatic rings [48]. The area near the chromophore region is the attacking site for the photodegradation of azo dyes resulting in the cleavage of azo bonds either symmetrically or asymmetrically [11].

Furthermore, based on the application, dyes are classified as water-soluble and insoluble as follows.

a. Water Soluble Dyes

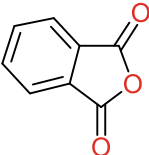
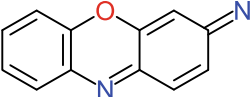
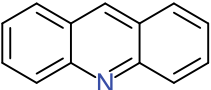
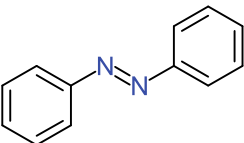
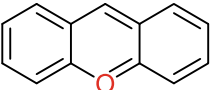
- Acid or Anionic dyes: These dyes are majorly utilized in the dyeing of fibres consisting of an amino group (NH_2) such as silk, polyamide and wool. Most of these dyes falls under the class of azo dyes and anthraquinone dyes.
- Basic or cationic dyes: These dyes possess the ability of directly imparting colour to the anionic sites-linked fibres. These dyes comprise of various chromophore groups falling under the class of azo, anthraquinone, triarylmethane, diarylmethane, anthraquinone.
- Reactive Dyes: It comprises of two vinylsulfone reactive groups and chromophore groups made from anthraquinone and azo dyes. Because of their stability, processing conditions and their greater ability to form covalent bonds with the fibres, reactive dyes are broadly used in the dyeing of cotton, silk and wool fibres.
- Direct or substantive dyes: For cellulose fibres, these dyes possess greater affinity and are significantly used for colouring paper products. Its chromophore grouping majorly includes azo and phthalocyanine.

Table 1 Dyes Classification based on Chromophore group [9, 10, 52, 54]

S. no.	Class	Chromophore
1	Phthalocyanine	
2	Nitro	
3	Anthraquinone	
4	Indigo	
5	Diphenyl Methane	

(continued)

Table 1 (continued)

S. no.	Class	Chromophore
6	Phthalein	
7	Oxazine	
8	Acridine	
9	Azo	
10	Xanthene	

b. Insoluble Dyes in Water

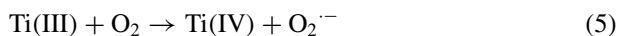
- **Vat dyes:** These dyes exhibit higher propinquity for cotton, rayon, silk, wool, cellulosic fibres and linen. Primarily possess solubility in hot water while few possess solubility in presence of sodium carbonate. Examples: Indigo carmine, Vat Yellow 1, Vat Black 25.
- **Sulphur dyes:** These dyes have similar use to vat dyes, contains sulphur-linked molecules produced from desulphurization of organic compounds, and are higher molecular weight dyes. Examples: Sulphur black and Sulphur blue 15.
- **Disperse dyes:** These are azo structure-based dyes and are mainly used for the dyeing of prefabricated fibres like polyamide and polyester with a suitable dispersing agent in the solution. Nano-sized disperse dye particles show good stability in the high-temperature dyeing process. Examples: Red Disperse 60, Blue disperse 7.

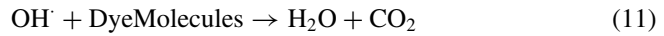
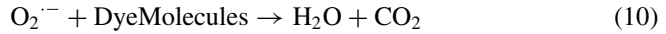
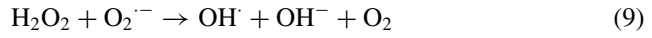
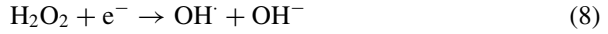
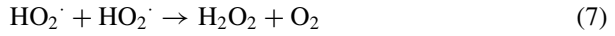
3 Dye Degradation Using Photocatalytic Membrane Reactor

3.1 Mechanism of Photocatalysis in Dye Removal from Aqueous Solution

The mechanism of the photocatalytic reaction is explained by considering TiO_2 as a photocatalyst. The photocatalytic reaction commences with Ultraviolet/Visible light irradiation having energy greater than the bandgap energy (E_g) of the TiO_2 photocatalyst (3.2 eV for anatase and 3.0 eV for rutile) [34, 69]. Upon irradiation, electrons present in the valence band absorb the energy, gets excited and migrates to the conduction band, leaving behind holes in the valence band. Photogenerated electrons then move to the catalyst surface and reduce the O_2 molecules present in the aqueous aerated solution or adsorbed O_2 molecules on the Ti(III) surface and convert them to superoxide radical ($\text{O}_2^{\cdot-}$) that can eliminate an extensive variety of dyes and can inactivate microorganisms. Oxygen molecule acts as an electron scavenger, and in its absence or shortage, photocatalytic reaction efficiency declines due to higher recombination of electrons and holes [3]. The recombination of charge species, i.e. electrons and holes results in the dissipation of heat [17].

Correspondingly, photogenerated holes take part in the oxidation reaction with H_2O and OH^- and converts them to hydroxyl radical (OH^\cdot) that acts as a strong oxidant and is responsible for the mineralization of organic compounds. Dye molecules adsorbed on the TiO_2 surface or are near to the catalyst surface are attacked by OH^\cdot non-selectively [2]. Superoxide radicals and protons react and produce hydroperoxide radicals (HO_2^\cdot) that exhibit greater potential for the generation of OH^\cdot , and this generated OH^\cdot produces the same effect as like $\text{O}_2^{\cdot-}$ [3, 41]. The pollutant concentration, irradiation time, loading of photocatalyst, presence of O_2 , pH of the aqueous solution, wavelength and irradiation intensity are the major factors that influence the photocatalytic reactions [45]. The reactions involved in the photocatalytic process are as follows.





Based on the above understanding of radical's generation and structural properties of dyes, an example of a possible photodegradation pathway of Acid Orange 7 dye is illustrated in Fig. 2.

3.1.1 Dye Sensitization

Generally, dyes are capable of absorbing visible light. Upon irradiation of visible light, dye molecules located at TiO_2 /solution interface get excited. From the excited dye molecules (Dye^*), electrons are ejected to the conduction band of TiO_2 and lead to the evolution of cationic dye radicals (Dye^+). The electron then participates in the redox reaction producing superoxide radicals ($\text{O}_2^{\cdot-}$) which in turn fosters the generation of hydroxyl radicals (OH^{\cdot}) that oxidizes the cationic dye radicals, and mineralized end products are formed [2] (Refer Fig. 3). To ensure effective ejection of an electron from the excited dye molecule (Dye^*) to the conduction band of TiO_2 , adsorption of dye molecules onto the TiO_2 surface should be strong enough. Adsorption of dye molecules can be influenced by varying the pH value of the solution as it alters the surface charge of the photocatalyst [34, 50]. The TiO_2 photocatalyst demonstrates a positive surface charge at pH less than 6.8 facilitating anionic dye attraction and cationic dye repulsion, whereas it exhibits opposite behaviour when pH is greater than 6.8 [34]. Therefore, it is evident that pH plays an important role in dye sensitization. Also, pH is one of the influential parameters in deciding the dye degradation efficiency. Therefore, the later section briefly discusses the performance of different configurations of photocatalytic membrane reactors for dye removal at varying pH values.



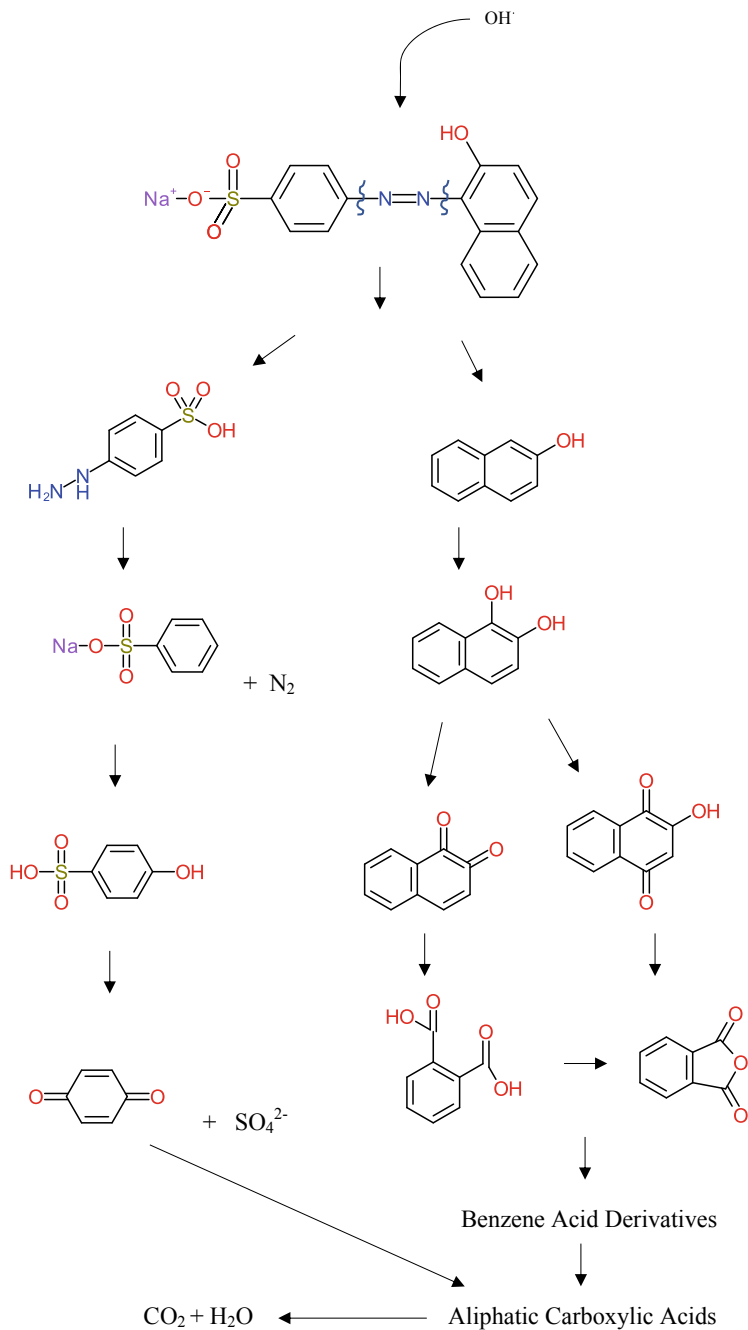


Fig. 2 Photodegradation pathway of Acid Orange 7 dye [63]

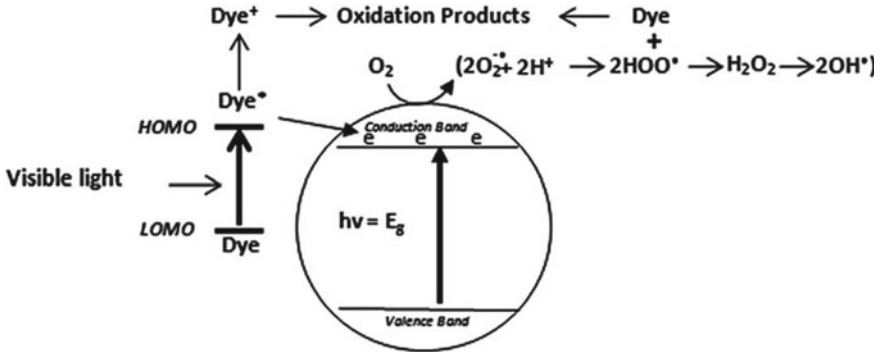
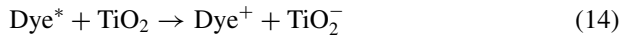


Fig. 3 Schematic illustration of Dye Sensitization [2]



3.2 Design of Photocatalytic Membrane Reactor (PMR)

The designing of a photocatalytic membrane reactor is one of the salient aspects that govern the dye removal efficiency and requires a fundamental understanding of material properties, membrane configuration and synthesis, pollutant behaviour, chemical formulation and reaction kinetics. The photocatalytic membrane reactor has gained widespread attention due to the photocatalytic reaction occurring at the surface of the membrane, which doubles the benefits by inhibiting the aggregation of photocatalysts, thus maintain the process, and lowering the membrane fouling tendency during the treatment processes. Furthermore, the photocatalytic membrane reactor operates in the continuous mode, and the membrane acts as a barrier that eases the separation of products, controls the mass transport, offers effective reaction time and contact area and improves photocatalyst recycling [8]. The generally employed membranes in PMR are MF, UF and NF [33]. The basic components controlling the performance of PMR are the light source, photocatalyst material and reactor design that includes the substrate material of membrane, and configuration of PMC. This section focuses on the characteristics and selection of substrate materials for the photocatalytic membrane along with their fabrication methods.

3.2.1 Substrate Material of Photocatalytic Membrane

The substrate material requires to provide chemical, mechanical, and thermal stability, high surface area and roughness to hold photocatalytic particles and flexibility in adding the functional groups. Generally, chemical composition and structure

influence permeability and selectivity of the membrane. Besides, morphology such as surface and cross-section makeup get altered when photocatalysts are introduced into the membrane matrix. Hence, based on these, the substrate material will be selected for the preparation of the membrane. Inorganic, organic and metallic materials are generally used in the photocatalytic membrane synthesis. The common organic material used for the membrane fabrication is polymers which include polyethylene terephthalate, polyamide, polyvinylidene fluoride, polyethersulfone, polyurethane, polyacrylonitrile and polytetrafluoroethylene. The resultant membrane is reported to be porous and having high surface roughness to offer high performance in dye removal. For instance, [23] demonstrated the intensification of membrane surface roughness with the increment of graphene oxide (GO) loading in graphene-dispersed polysulfone-mixed matrix membrane (PSf/GO). The study witnessed that the hydrophilic GO exhibits a higher affinity towards water, leading to fast migration of GO-dispersed N-methyl-2 pyrrolidone solvent into non-solvent water during the phase inversion process. This resulted in the formation of a sphere or nodule of polymer that was attributed as a surface roughness (mean fit = 2.35 μm) which further increased the membrane porosity.

Considering the damages associated with the irradiation, and redox reactions due to the direct interaction of membrane with the reaction environment, inorganic ceramic materials such as Al_2O_3 , TiO_2 , SiO_2 , ZrO_2 are the most viable substrate materials compared to polymeric materials. Furthermore, the ceramic membrane possesses higher chemical, mechanical, and thermal stability, a long life span and demonstrates good antifouling properties but is expensive comparatively [6, 26].

The dye removal studies carried out using different varieties of the membrane substrate material in PMR are compiled in Table 2.

3.2.2 Fabrication of Photocatalytic Membrane

Designing and modification in coherence with advancement towards commercialization of photocatalytic membrane reactor requires a deeper understanding of membrane fabrication methods. Therefore, this section emphasizes the mechanism, operation, components and governing factors involved in the different membrane fabrication methods that are prevalent or are recently developed.

Dip Coating

The dip-coating is one of the easiest and widely used methods for immobilizing photocatalyst particles onto the membrane surface [4]. The dip-coating method encompasses immersion of a membrane substrate at a specific speed into the coating solution containing photocatalyst particles. On the membrane surface, the complete deposition of particles is ensured by providing full penetration of the substrate material at an optimum speed for its complete wetting, sufficient contact time and then withdrawing at a constant speed. This is followed by evaporation of solvent leading to the development of a thin film on the surface [57, 61]. The morphology and the thickness of the deposited film are greatly influenced by the viscosity, density, surface

Table 2 Removal of pollutants using different varieties of the membrane

S. no.	Membrane type	Pollutant removal	References
1	Cr ₂ O ₃ -enriched geopolymer-based photocatalytic membrane (Cr ₂ O ₃ /GPCM)	Basic Green Dye	[14]
2	Ag ₃ PO ₄ /Graphene Oxide/3-aminopropyltriethoxysilane/PVDF composite membrane	Rhodamine B and Methylene Blue	[14]
3	N-vinylcaprolactam-TiO ₂ -acrylic acid (VCL-TiO ₂ -AA) polymer nanocomposite modified polysulfone ultrafiltration membrane	Methylene Blue	[58]
4	AgCO@UiO/Graphene Oxide membrane	Rhodamine B, Methylene Blue, Methyl Red	[68]
5	N-doped TiO ₂ -ZrO ₂ /TiO ₂ composite ultrafiltration membrane	Methyl Orange	[14]
6	Meso-tetrakis (1-methylpyridinium-4-yl) porphyrin-immobilized sulfonated polysulfone/polyethersulfone blend membrane (TMPyP@SPSf/PES)	Rhodamine B	[65]
7	Cadmium sulphide/polymethyl methacrylate nanocomposite membrane (CdS/PMMA)	Rhodamine B	[28]
8	TiO ₂ -coated polyvinylidene fluoride flat sheet membrane (PVDF)	Reactive Blue 19	[51]
9	g-C ₃ N ₄ /TiO ₂ composite photocatalyst/polyacrylic acid/polytetrafluoroethylene ultrafiltration membrane (CNTO/PAA/PTFE UFM)	Methylene Blue	[16]
10	Composite membrane -Polysulfone/Nitrogen, Palladium co-doped TiO ₂	Eosin Yellow degradation	[38]
11	Multi-wall carbon nanotubes/Ag ₃ PO ₄ /polyacrylonitrile (PAN) ternary composite fibre membrane	Rhodamine B	[66]
12	Graphene oxide/polyacrylonitrile composite membranes (GO/PAN)	Indigo, Methylene Blue, Thymol Blue, Congo Red	[22]
13	Acrylonitrile butadiene styrene/polyurethane blend membrane (ABS/PU)	Disperse Yellow 23, Disperse Red 60, Disperse Yellow 23, Disperse Blue 183, Vat brown 55, Vat blue 66 and Vat red 10	[42]

(continued)

Table 2 (continued)

S. no.	Membrane type	Pollutant removal	References
14	TiO ₂ /α-Al ₂ O ₃ porous membrane	Methylene Blue	[43]
15	Polysulfone/Titanium dioxide/Multi-walled carbon nanotubes mixed matrix Membranes (PSF/TiO ₂ /MWCNT)	Acid Black 1	[35]
16	Polyvinylidene fluoride/meso-TiO ₂ hybrid membrane	Methyl Orange	[64]

tension and evaporation conditions of the coating solutions along with the immersion time, withdrawn speed, dip-coating cycle and substrate surface characteristics. Various dip coating methods so far followed are direct solution dipping, multi-layered dip coating, photo-based, spin-based, sol-gel-based and vacuum-based methods. The dip-coating method can be operated continuously and is usually employed for ceramic membrane preparation [18]. The availability of quality photocatalyst powder in the photocatalytic membrane to the dyes is the vital deciding factor that controls the removal efficiency. For example, TiO₂-coated polyvinylidene fluoride (PVDF) membrane was fabricated using dip coating with a contact period of 5–60 min. It was observed that membrane porosity declined with an increase in contact period due to aggregation of TiO₂ photocatalyst particles leading to blockage of pores. In addition, the dye removal efficiency escalated from 57.09% to 86.1% with an increment in photocatalyst loading from 0.1 to 1 g/L because of the increase in active sites [51].

Spin Coating

In this method, on the surface of the planar membrane substrate, thin and uniform polymer films are deposited. The various steps involved in the spin coating method are deposition, spin-up, spin-off and evaporation. Initially, the substrate is placed on the revolving base known as a spinner. Either at static or at a slow speed of revolving spinner, the deposition of the photocatalytic solution takes place on the centre of the substrate's surface, and this is known as deposition step. At the spin-up step, the deposited solution spreads radially outward due to centrifugal force exhibited by the high-speed revolving spinner. In spin-off step, accumulation and ejection of the solution takes place due to its outward flow towards the perimeter. The last step involves thinning up the solution due to evaporation, leaving behind the photocatalyst film on the surface of membrane. Various factors influencing the film thickness are evaporation rate, angular velocity, volatility and diffusivity of the solvent along with the solution concentration and its viscosity [20]. The advantage of the spin coating method is that it is applicable for organic, inorganic and organic–inorganic solution mixtures [49].

Electrospinning and Electrospraying

Using electrospraying and electrospinning, the photocatalytic membrane itself can be created or the coating of photocatalyst on the membrane can also be achieved.

The basic principle here is—a high electric field is applied on a blend solution that produces photocatalyst (or membrane substrate and photocatalyst) nanofibres which gets settled on a collector. In case of photocatalyst coating, the membrane substrate will be placed on the collector. The key components of the electrospinning setup are (i) syringe with a needle containing the solution, (ii) high voltage power source and (iii) flat or drum type collector. Initially, the syringe is filled with blend solution, and the metallic needle is applied with high voltage to produce an electric field to vanquish the surface tension of the solution leading to the development of cone-shaped droplet at the needle tip. The syringe pump then constantly pushes the solution, producing ultrafine fibre that gets collected on the collector or the surface of membrane.

The electrospinning are of different configurations such as melt, single-spinneret, multi-spinneret and co-axial [62]. Nano-fibres of polymers, metals, composites and ceramics can be produced by this method. Electric field intensity, solution viscosity and flow rate, polymer concentration, air humidity and work distance influence the electrospinning process [31]. Electro spraying and electrospinning only differ in the quantum of polymer chain entanglements and their presence in the solution. Simply, by lowering the polymer chain entanglements in the solution, structure of regular nanofibres can be transformed to beaded nanofibres and to particles under identical electrospinning conditions [39]. The membrane fabricated using electrospinning demonstrates higher surface area to volume ratio and higher permeability due to its immense control on the cross-linking and regularity.

Vacuum Filtration

Vacuum Filtration allows the photocatalyst particles deposition onto the membrane surface physically. By controlling the concentration of the photocatalyst particles and pressure of the vacuum, different loads of photocatalyst particles can be deposited onto the membrane surface. The large thickness and higher density membrane can be achieved using this method. The uniformity in coating largely depends on the downstream vacuum pressure. This method requires well-dispersed photocatalytic particles, else a non-uniform photocatalytic membrane will be formed due to aggregation of particles. Various photocatalyst particles used in the fabrication of photocatalytic membrane are MoS₂ nanosheets, graphitic carbon nitride and graphene using this method [15].

Phase Inversion

Under controlled conditions, phase inversion refers to the phase transformation of the stable thermodynamic polymer solution from liquid to a solid phase. In other words, precipitation of a polymer from a layer of casting solution involves a change to the solid phase from the solution phase of the polymer by suitable manipulation of the environment. Various techniques of phase inversion are precipitation by immersion in a non-solvent, precipitation by cooling and precipitation by evaporation [21, 27].

In case of immersion in a non-solvent, the cast solution comprising of a membrane substrate (and photocatalyst) in a solvent is immersed in a coagulation tank consisting of non-solvent. The membrane (with the photocatalyst) is precipitated due to the migration of material from the solvent to the non-solvent side. This results in the

formation of a dense ultrathin skin (containing the photocatalyst) at the exposed surface. This dense layer depresses the rate of migration of solvent inside the surface which further lowers the precipitation and forms larger pores. This results in the formation of an asymmetric membrane comprising of dense ultrathin skin layer with porous substructure. Symmetric membranes can also be fabricated by this method by controlling the migration rate of the solution.

In precipitation by cooling method, on any desired surface, the solution containing membrane substrate material (and photocatalyst) and solvent is casted and allowed to cool. The solubility of the solution decreases as the layer cools and formation of a film matrix takes place. Polymeric membranes prepared by this method are polypropylene, polyethylene, polysulfone, polyvinylidene fluoride. In the case of precipitation by evaporation, solvent or mixture of the solvent evaporates from a cast solution, due to which solubility of the solution decreases and precipitation of the solution material occurs. Dense anisotropic membranes with or without photocatalyst can be obtained by this method [21].

3.2.3 PMR Configurations

The photocatalytic membrane process is the compilation of advanced oxidation process with the separation process. To get the most efficiency on the dye removal, the configuration of the PMR is vital. The configurations of PMR are mainly categorized into two (i) photocatalyst in suspension inside the membrane reactor (ii) photocatalyst implanted or immobilized on the membrane surface inside the reactor. The active surface area available for the pollutants is more in the suspended catalyst system as compared to the immobilized catalyst ensuring higher photocatalytic performance for the former and a portion of loss in photoactivity at the latter case. Furthermore, the drawback of the suspended catalyst reactor is the difficulty in recovering or removing the particles after the decontamination of wastewater, whereas an immobilized catalyst reactor eliminates this requirement [44, 46]. Correspondingly, photocatalyst in immobilized mode should be stable and must exhibit strong adhesion with the membrane material. Impregnation of catalyst within the membrane has better reusability and recoverability at nominal cost [44]. Reference [65] fabricated a mesotetrakis (1-methylpyridinium-4-yl) porphyrin-immobilized sulfonated polysulfone/polyethersulfone blend membrane (TMPyP@SPSf/PES) for the degradation of Rhodamine B and Methylene blue dye under visible light (300 W), and has observed the degradation efficiency upto 98.3% and 99.1% for Rhodamine B and Methylene blue dye, respectively.

The studies on PMR for the removal of dyes used varieties of PMR configurations as follows. Figure 4a represents the suspended photocatalyst PMR with the light source placed above the membrane matrix, whereas in Fig. 4b, light source is placed above the feed chamber. Moreover, light source can also be placed both above the feed chamber and membrane matrix. Also, a light source can be placed inside the feed solution using immersed lamps. Figure 5 represents the PMR with photocatalyst embedded on and within the membrane.

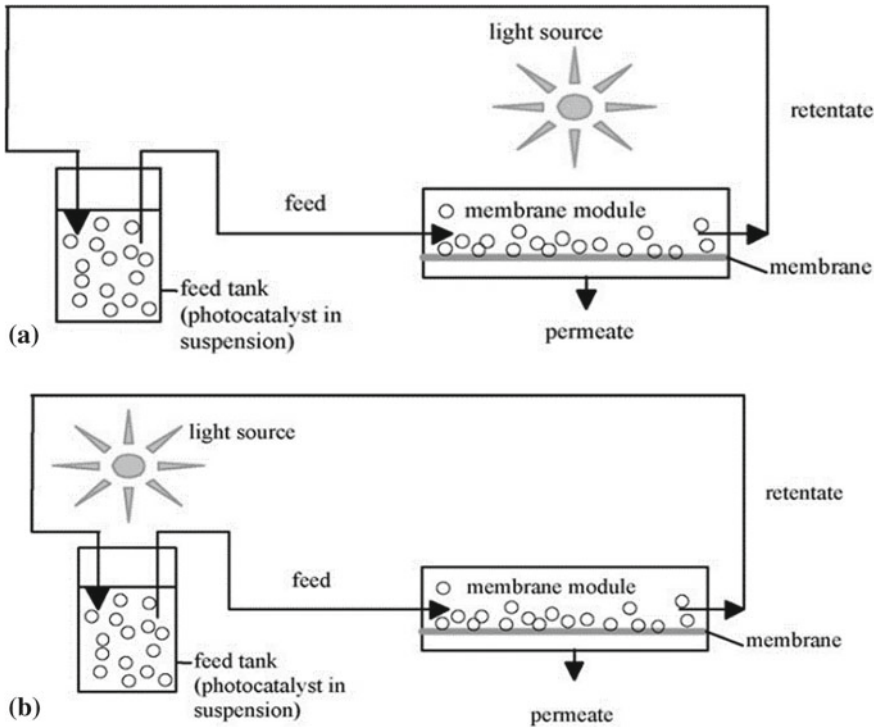


Fig. 4 Suspended PMR **a** Illumination of Membrane Matrix **b** Illumination of Feed Tank [46]

Slurry-Based Photocatalytic Reactor

Slurry-Based Photocatalytic Reactor offers larger interaction between the contaminants and the photocatalyst suspended in the slurry, and are coupled with membrane matrix for separation purposes. Depending upon the configuration, two types of slurry-based photocatalytic reactor are (i) Split-type (ii) Integrated Type. In the case of Split-type, photocatalytic oxidation and membrane separation take place in different chambers as shown in Fig. 6a), whereas both occur in the same chamber in the case of Integrated type [37]. [12] conducted an experiment for the eradication of Disperse Red 73 (DR73) dye from the textile industry effluents using TiO_2 suspended photocatalytic reactor combined with hollow fibre micro-filtration membrane module under ultraviolet irradiation (24 W UV Lamp). Measurement of the percentage of dye degradation was based on the efficiency of Chemical Oxygen Demand (COD) removal. The analysis revealed that the COD removal efficiency elevates from 70 to 90% with an increase in TiO_2 loading from 0.5 g/L to 2 g/L after 180 min of treatment due to an increase in photocatalytic activity as active site increases (Refer Fig. 6b).

Reference [19] carried out an experiment for the elimination of reactive black 5 dye using an integrated type slurry-based photocatalytic reactor built by immersing

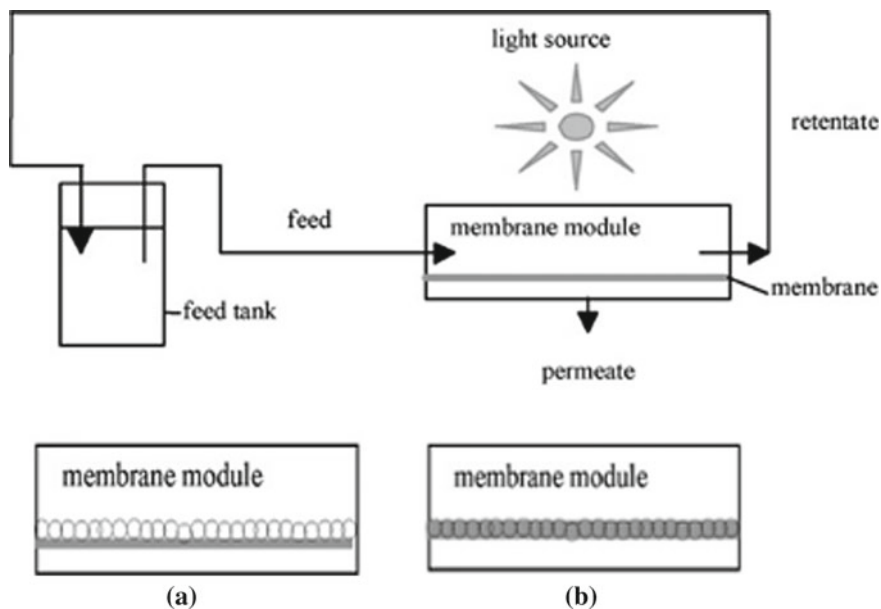


Fig. 5 Immobilized PMR **a** Embedded on the Membrane **b** Within the Membrane [46]

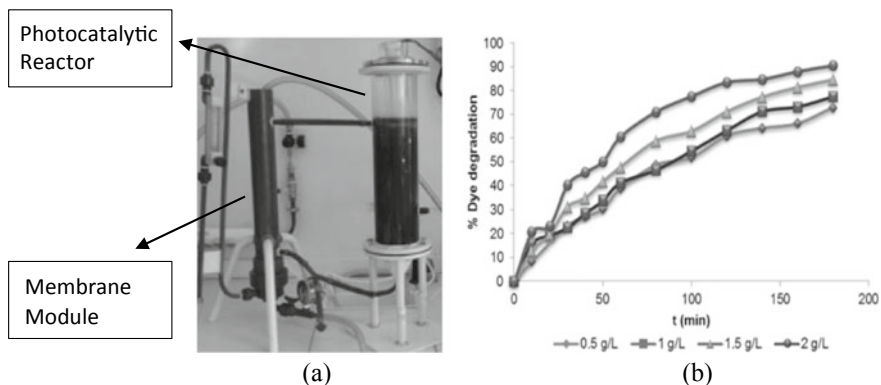


Fig. 6 Split-type Photocatalytic Membrane Reactor **a** Experimental Setup **b** % Dye Degradation Versus time (in min) [12]

a flat polytetrafluoroethylene (PTFE) membrane module into a TiO₂-based slurry photocatalytic reactor as illustrated in Fig. 7a. The membrane module was positioned at the middle of the container and in between the two Ultraviolet lamps (15 W each). Furthermore, a magnetic stirrer was used for mixing the solution along with the air diffuser for continuous aeration. Measurement of % dye degradation was based on COD and Total Organic Carbon (TOC) removal. Experimental results reveal

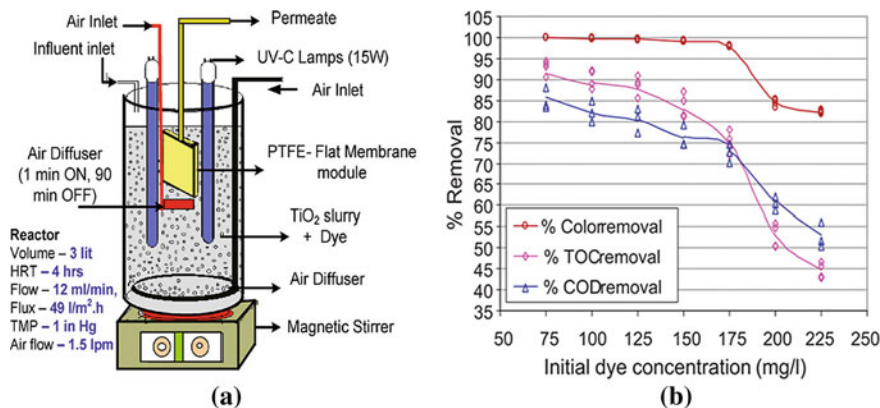


Fig. 7 Integrated Slurry PMR **a** Experimental Setup **b** % Removal versus Initial Dye Concentration [19]

that under continuous flow PMR having a detention period of 4 h, the percentage removal of TOC, COD and colour decreases from 92 to 46%, 82 to 56%, 99.3 to 83%, respectively, with the surge in initial concentration of dye (Refer Fig. 7b). This is because a higher initial concentration of dye intensifies the colour of the solution thereby affecting the depth of the UV light penetration. Moreover, due to constant light intensity and irradiation time, the energy available for the radical generation declines with mounting dye concentration as dye molecules absorb the photon flux.

Immobilized Photocatalytic Membrane Reactor

In this configuration, the membrane not only acts as a selective barrier for the pollutants, but also serves as a support for the photocatalyst [45]. Based on the integration of the photocatalyst, the immobilized PMR are categorized into three types, (i) Membrane coated with photocatalyst (ii) Blending of photocatalyst with the membrane (iii) Self-Photocatalytic membrane.

Membrane Coated with Photocatalyst

Coating techniques like magnetron sputtering, dip-coating, chemical vapour deposition (CVD) and atomic layer deposition (ALD) and electrospinning and electro-spraying are used for the synthesis of photocatalytic membranes [37]. A laboratory-scale experiment was carried out by [5] for methylene blue removal using nanofibre membranes deposited with titania nanoparticles. The membrane was fabricated using electrospinning and electro-spraying. The study incorporates two cases, i.e. batch process and continuous process for the deposition of nanoparticle and nanofibre as demonstrated in Fig. 8. It was observed that the percentage degradation of methylene blue after 90 min of treatment under UV irradiation ($0.6\text{mW}/\text{cm}^2$) is 65.48% for batch process and 99.6% for continuous process, inferring that the batch process membrane fabrication is less efficient as compared to the continuous process because of the

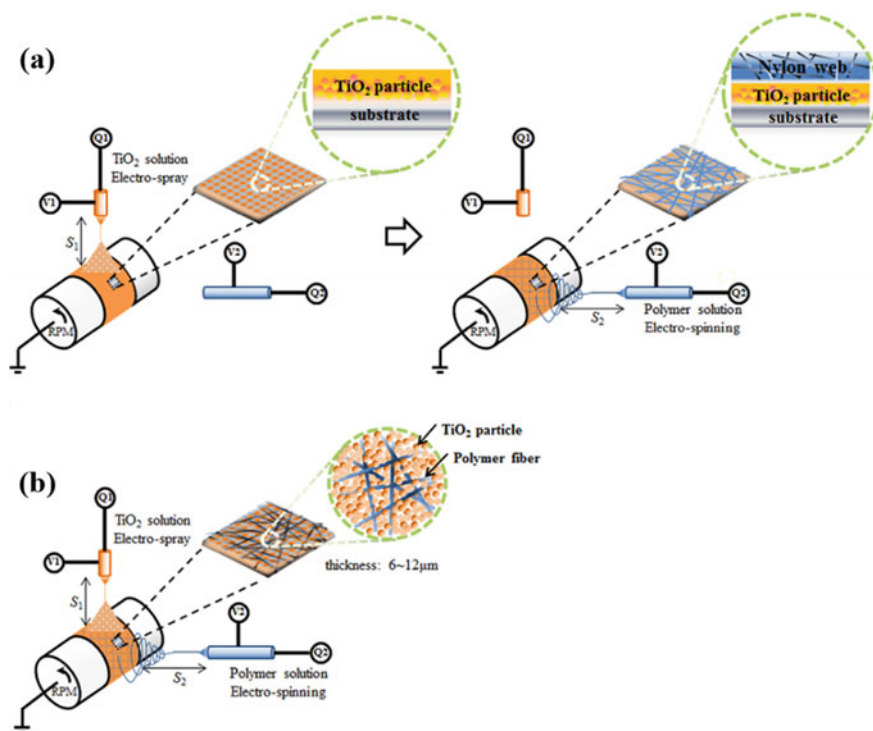


Fig. 8 Photocatalytic membrane fabrication method **a** batch process and **b** continuous process [5]

reduction in photoactive interfacial area due to bilayer deposition of nanoparticles and nanofibres.

Photocatalytic activity of TiO₂-coated Polyvinylidene fluoride membrane synthesized by sol–gel method was tested for the Reactive Black 5 (RB5) dye degradation under ultraviolet illumination (UV-C, 15 W). The TiO₂ particles in this experiment were synthesized at specific pH value 1, 1.25, 1.5 and have found percentage degradation of 54.58, 98.77 and 30.12% for Reactive Black 5 dye in 5 h at pH value of 1.5, 1.25, 1, respectively. This is because of higher photocatalytic activity at pH 1.25, because of high sol density compared to pH 1.5 and due to origination of more favourable TiO₂ crystal type at pH 1.25 than pH 1 [36].

Blending of Photocatalyst with the Membrane

Wet spinning, nonsolvent-induced phase separation (NIPS), electrospinning and sintering are the methods used for the synthesis of these types of membrane. The major advantage of these types of membranes is that the leaching of photocatalyst gets curtailed. Optimizing the proportion of the photocatalyst and the membrane precursors can help us to get the required stability and reactivity of the membrane [37]. Reference [53] carried out an experiment to investigate the effect of photocatalytic

dye degradation under varying experimental conditions like irradiation time, initial concentration of dye and pH using zinc oxide-blended cellulose acetate-polyurethane (CA-PU/ZnO) membrane prepared using solution dispersion blending method for removal of Reactive Red (RR 11) and Reactive Orange (RO 84) dyes. Moreover, in this experiment, ZnO nanoparticles were synthesized by sol gel method. Figure 9 illustrates the experimental setup in which funnel contains the prepared membrane with dye solution and at different time intervals (10–60 min) kept under the sunlight. It was found that with increase in illumination time, the degradation efficiency of dye escalates and reaches its peak after 40 min and then remains constant. Therefore, illumination time of 40 min is kept fixed for the study. It was also observed that at pH value 7, higher degradation efficiency of RR11 and RO84 dyes was achieved by CA-PU/ZnO membrane. Neutral pH is well suited for better performance, because at low pH, ZnO reacts with acids to produce salts, whereas it forms complexes after reacting with base at high pH value. Correspondingly, analysis discovered that the dye degradation efficiency declined with increase in initial dye concentration from 50 to 250 mg/L because generation of hydroxyl ion decreases as active sites of the photocatalyst gets shrouded with the dye molecules.

Reference [1] utilizes the Metal–organic frameworks (MOFs) for the photocatalysis and demonstrated the photocatalytic degradation of methylene blue dye over 5 h under dark, ultraviolet ($\lambda = 253.7$ nm, 6 W) and visible irradiation ($\lambda > 420$ nm, 6 W) using Polysulfone-Blended NH_2 -MIL125 (Ti) membrane with MOF/PSf percentage composition of 0, 0.2, 0.5 and 1 wt% and fabricated through phase inversion method.

The NH_2 -MIL125(Ti) is a metallic organic form with cyclic $\text{Ti}_8\text{O}_8(\text{OH})_4$ oxo clusters and 2-aminoterephthalate ligands and exhibit greater adsorption affinity towards visible light due to the presence of amino-functionalized structure. For the analysis, membrane polymeric strip (8 cm x 8 cm) was suspended in 100 mL of methylene blue solution having concentration 10 ppm (Refer Fig. 10). At an interval of 60 min, 2 mL

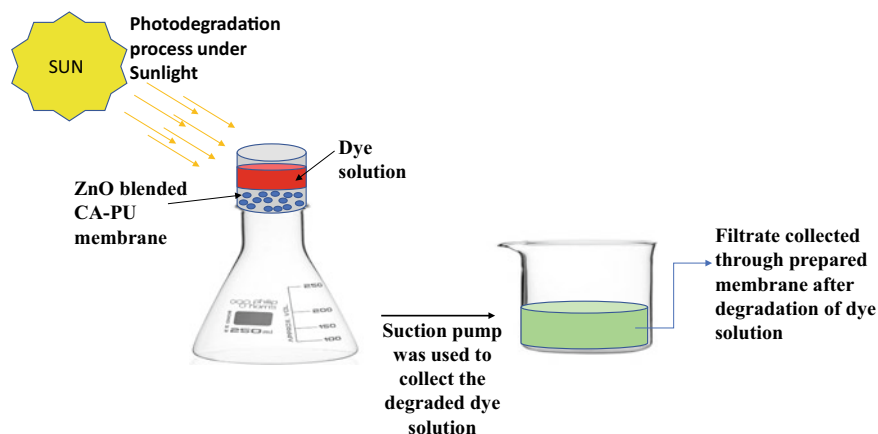


Fig. 9 Experimental Setup for Dye Degradation using CA-PU/ZnO membrane [53]

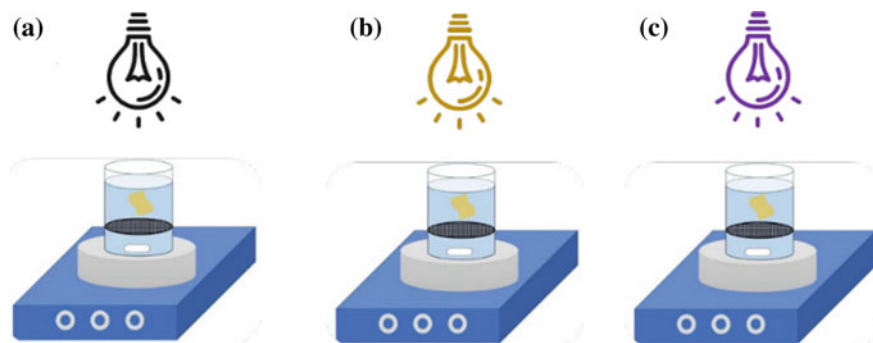


Fig. 10 Experimental Setup in **a** dark, **b** Visible light and **c** UV light [1]

aliquots of the dye solution are withdrawn with a disposable syringe and were monitored using UV–Vis Spectrophotometer. Higher dye removal percentage was found in $\text{NH}_2\text{-MIL125(Ti)/PSf}$ membrane with composition 1% (in weight) under all three conditions, i.e. dark, visible as well as ultraviolet irradiation. $\text{NH}_2\text{-MIL125(Ti)/PSf}$ membrane with composition 0, 0.2, 0.5 and 1 wt% showed 30.840, 36.779, 44.203, 49.268% dye removal, respectively, under visible irradiation, whereas under ultraviolet irradiation, they showed 38.538, 48.846, 52.076 and 56.076% dye removal, respectively. This is due to the fact that with increasing concentration of $\text{NH}_2\text{-MIL125(Ti)}$, the density and the quantity of membrane pores got enlarged gradually. Furthermore, under dark conditions, due to the adsorption dominance in the dye degradation, $\text{NH}_2\text{-MIL125(Ti)/PSf}$ membrane with composition 0, 0.2, 0.5 and 1 wt% showed 26.145, 27.389, 31.592 and 37.881% dye removal, respectively.

Self-Catalytic Membrane

These membranes are constructed with a pure photocatalyst through electrochemical anodization, and do not necessitate any immobilization step as required in the coated or blended membrane and can act as antifouling membranes. These membranes possess higher hydrophilicity, anatase crystallinity and surface area and significantly lowers the tendency of photocatalyst leaching [6, 37]. Fabrication of TiO_2 membrane using electrochemical anodization of titanium metallic substrate is widely used, as anodization favours the growth of TiO_2 nanotube from the oxidized Titanium electrode in the presence of fluoride ions in an aqueous electrolytic solution [30, 37].

4 Selected Case Studies

This section delineates the recent pilot-scale studies undertaken by the researchers for dye removal. The following case studies intend to develop a framework and to understand the characteristics and behaviour of different reactor setups.

4.1 Photocatalytic Membrane Bioreactor (PMBR)

Reference [56] experimented to explore the efficiency of tungsten oxide with graphene oxide alginate beads (WO_3/GO) for the photocatalytic degradation of dye using hollow fibre polyethersulphone membrane bioreactor under visible irradiation. Modified Hummer Method was used for the Graphene Oxide synthesis. Synthesis of tungsten oxide involves the usage of tungsten oxide powder, polyvinylpyrrolidone, sodium alginate and calcium chloride bath. Textile wastewater was pumped with a flowrate of 6.7L/h into the photocatalytic reactor having a contact time of 3 h. At the bottom surface of the photocatalytic reactor, an aerator was placed for homogenous mixing of the solution. Furthermore, from the top of the photocatalytic reactor, visible light of 500 W was immersed, reaching $\frac{3}{4}$ th of the tank. The wastewater after photocatalysis passes to the membrane bioreactor (refer Fig. 11). In membrane bioreactor, a hydraulic retention time of 10 h and mixed liquor suspended solid concentration of 8000 mg/L was maintained. The experiment was run twice using both tungsten oxide (WO_3) as well as tungsten oxide (WO_3) with graphene oxide (GO) alginate beads in the photocatalytic reactor. Under the catalyst loading of 500 mg/L and reaction time of 3 h, the analysis of the photocatalytic reactor effluent revealed that a higher percentage of colour and COD removal was found in the case of WO_3/GO , i.e. 25 and 44%, respectively, whereas in the case of WO_3 , it was 21 and 36%, respectively. The higher efficiency of WO_3/GO is because graphene oxide acts as an electron acceptor, and it lowers the recombination of electrons and holes resulting in a higher dye degradation efficiency. The effluent from the membrane bioreactor shows 76% COD and 70% colour removal due to higher biomass growth ensuing integrated PMBR improves the degradation efficiency.

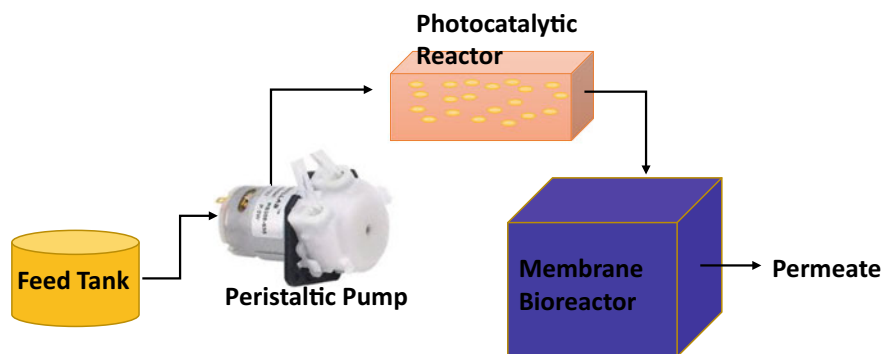


Fig. 11 Experimental Setup of Photocatalytic Membrane Bioreactor (PMBR)

4.2 C-TiO₂-CFA/PAN Photocatalytic Membranes

Reference [47] demonstrated the removal of golden yellow and methyl orange textile dyes using novel polyacrylonitrile membrane supported carbon-doped titanium dioxide-coal fly ash nanocomposite (C-TiO₂-CFA/PAN). Optimization of photocatalyst along with the effect of pH, photocatalyst loading (0%, 1%, 1.5% and 2% C-TiO₂-CFA), initial dye concentration was also evaluated. The carbon-doped titanium dioxide-coal fly ash nanocomposite was synthesized by sol-gel method and through phase inversion technique, immobilized on polyacrylonitrile membrane. Scanning electron microscope analysis reveals the fabricated membrane to be asymmetric with a thin top layer and porous sub-layer. Optimization of photocatalyst for degradation of dyes with different ratios of C-TiO₂: CFA is illustrated in Fig. 12.

Figure 12 infers that the optimum proportion of C-TiO₂:CFA is 4:1 having a degradation efficiency of 70.5% for Methyl Orange and 93.8% for Golden Yellow dye in 180 min. The degradation efficiency of 90.30% for methyl orange and 89.90% for golden yellow was achieved by using photocatalyst loading of 2% C-TiO₂-CFA/PAN, ensuing increase in photocatalyst loading leads to increment in photocatalytic dye degradation. Also, it was noticed that the degradation efficiency declines with the rise in initial dye concentration because of solution opacity as illustrated in Fig. 13. Furthermore, higher photocatalytic activity was observed at lower pH. This is because the TiO₂ photocatalyst surface exhibits a positive charge, and methyl orange and golden yellow dye under acidic conditions exhibit zwitterionic structure, because of

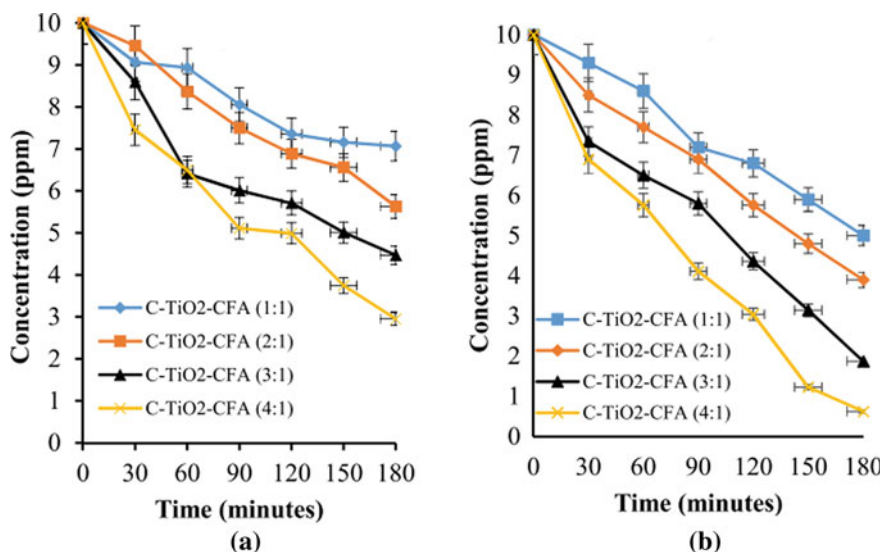


Fig. 12 Degradation of **a** Methyl Orange **b** Golden Yellow dye with different proportion of C-TiO₂:CFA [47]

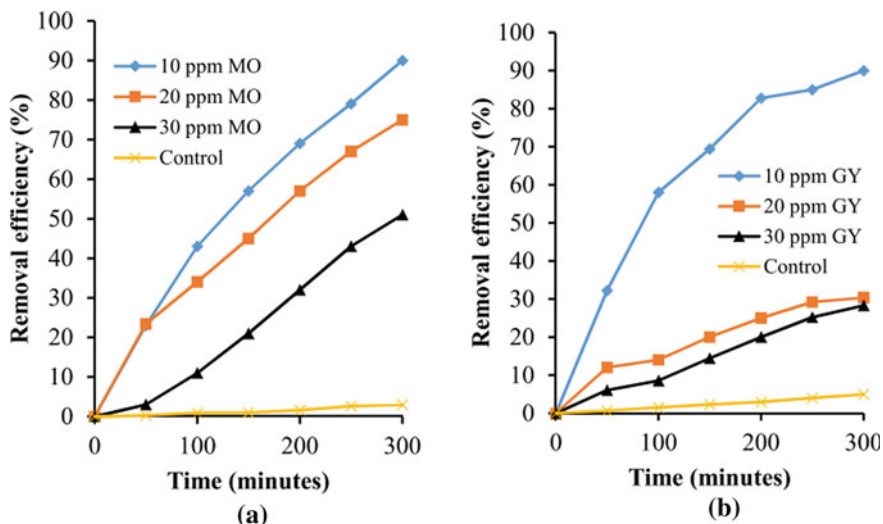


Fig. 13 Removal Efficiency (%) versus Time with increase in initial dye concentration **a** Methyl Orange **b** Golden Yellow dye [47]

which adsorption of dyes on the photocatalyst surface is enhanced leading to a higher rate of photodegradation of dyes.

4.3 Solar Photocatalytic Membrane Reactor with Fe^{3+} -Doped ZnO/polyester

Reference [7] investigated the photocatalytic degradation of Reactive Blue 5 (RB5) dye using Fe^{3+}/ZnO /polyester-based solar PMR. The experiment was performed in a borosilicate glass container comprising of 100 ml of RB5 dye solution (30 ppm), $5cm^2$ swath of $Fe^{3+}/ZnO/PMR$ and ZnO/PMR with 60 mg as an average catalyst loading and 30 Mm of H_2O_2 concentration at pH 7 with D65 cool artificial daylight tubes (72 W) under 30–35 °C. Results reveal that untreated dye, i.e. blank showed no change in concentration with time. $Fe^{3+}/ZnO/PMR$ showed maximum dye degradation efficiency in 180 min treatment because doping of Fe^{3+} with ZnO reduces the bandgap resulting in a higher rate of hydroxyl radical generation (refer Fig. 14). Also, the higher photocatalytic activity of $Fe^{3+}/ZnO/PMR$ was observed due to its ability to harvest a visible spectrum of irradiation along with an increased rate of dye adsorption due to higher surface roughness and hydrophilicity.

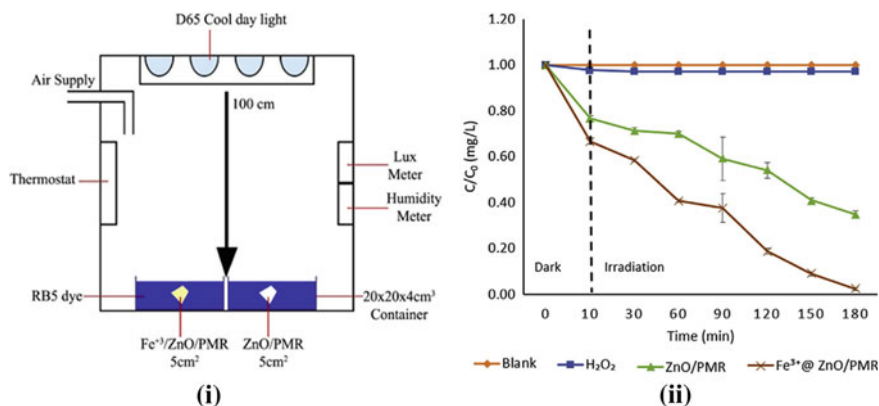


Fig. 14 (i) Experimental Setup of Fe³⁺/ZnO/polyester-based solar PMR (ii) Degradation of Reactive Blue 5 Dye with time [7]

5 Conclusion

The photocatalytic membrane reactor is gaining widespread recognition due to its broad-spectrum applicability and inherent advantages like low operational cost, low membrane fouling, anti-bacterial properties and efficient degradation of dye effluents. Due to several drawbacks associated with the suspended catalyst system, immobilization of photocatalyst has significant importance in practical applications. Excessive photocatalyst loading reduces the photocatalytic activity due to solution opacity. Commercial application of photocatalytic membrane technology should be promoted by performing pilot-scale experiments or projects. Studies should focus on the discovery of novel visible light-responsive photocatalyst for the elimination of organic contaminants and their suitable recovery/reuse method. Furthermore, an investigation should also be made for the development of advanced membrane material to ensure its stability under UV irradiation and to lower the membrane resistance, and concentration polarization.

Acknowledgements Dr. Ambika S would like to acknowledge the Science Engineering and Research Board (SERB), India for their funding support under Start up Research Grant (File Number: SRG/2020/000793) and Seed Grant (letter dated 15.5.2020) from Indian Institute of Technology Hyderabad, India.

References

1. Ahmadi A, Sarrafzadeh MH, Mohamadi M, Mahdigholian Z, Hosseinian A (2020) Investigation on polysulfone blended NH₂-mil125 (Ti) membrane for photocatalytic degradation of

- methylene blue dye. *J Water Environ Nanotechnol* 5:234–245. <https://doi.org/10.22090/jwent.2020.03.004>
2. Ajmal A, Majeed I, Malik RN, Idriss H, Nadeem MA (2014) Principles and mechanisms of photocatalytic dye degradation on TiO₂ based photocatalysts: a comparative overview. *RSC Adv* 4:37003–37026. <https://doi.org/10.1039/c4ra06658h>
 3. Al-Mamun MR, Kader S, Islam MS, Khan MZH (2019) Photocatalytic activity improvement and application of UV-TiO₂ photocatalysis in textile wastewater treatment: a review. *J Environ Chem Eng* 7.<https://doi.org/10.1016/j.jece.2019.103248>
 4. Alias NH, Nor NAM, Mohamed MA, Jaafar J, Othman NH (2020) Photocatalytic materials-based membranes for efficient water treatment. *Handbook of Smart Photocatalytic Materials*. INC. <https://doi.org/10.1016/b978-0-12-819051-7.00007-5>
 5. An S, Lee MW, Joshi BN, Jo A, Jung J, Yoon SS (2014) Water purification and toxicity control of chlorophenols by 3D nanofiber membranes decorated with photocatalytic titania nanoparticles. *Ceram Int* 40:3305–3313. <https://doi.org/10.1016/j.ceramint.2013.09.104>
 6. Argurio P, Fontananova E, Molinari R, Drioli E (2018) Photocatalytic membranes in photocatalytic membrane reactors. *Processes* 6.<https://doi.org/10.3390/pr6090162>
 7. Ashar A, Bhatti IA, Ashraf M, Tahir AA, Aziz H, Yousuf M, Ahmad M, Mohsin M, Bhutta ZA (2020) Fe³⁺ @ ZnO/polyester based solar photocatalytic membrane reactor for abatement of RB5 dye. *J Clean Prod* 246.<https://doi.org/10.1016/j.jclepro.2019.119010>
 8. Basile A, Sylwia Mozia, Raffaele Molinari (2018) Current trends and future development on bio membranes photocatalytic membranes and photocatalytic membrane reactors, Elsevier
 9. Benkhaya S, M'rabet S, El Harfi A (2020) A review on classifications, recent synthesis and applications of textile dyes. *Inorg Chem Commun* 115:107891. <https://doi.org/10.1016/j.inoche.2020.107891>
 10. Berradi M, Hsissou R, Khudhair M, Assouag M, Cherkaoui O, El Bachiri A, El Harfi A (2019) Textile finishing dyes and their impact on aquatic environs. *Heliyon* 5.<https://doi.org/10.1016/j.heliyon.2019.e02711>
 11. Bilal M, Rasheed T, Iqbal HMN, Yan Y (2018) Peroxidases-assisted removal of environmentally-related hazardous pollutants with reference to the reaction mechanisms of industrial dyes. *Sci Total Environ* 644:1–13. <https://doi.org/10.1016/j.scitotenv.2018.06.274>
 12. Buscio V, Brosillon S, Mendret J, Crespi M, Gutiérrez-Bouzán C (2015) Photocatalytic membrane reactor for the removal of C.I. disperse red 73. *Materials (Basel)*. 8:3633–3647. <https://doi.org/10.3390/ma8063633>
 13. Chang MW, Chung CC, Chern JM, Chen TS (2010) Dye decomposition kinetics by UV/H₂O₂: Initial rate analysis by effective kinetic modelling methodology. *Chem Eng Sci* 65:135–140. <https://doi.org/10.1016/j.ces.2009.01.056>
 14. Chen H, Zhang YJ, He PY, Li CJ, Li H (2020) Coupling of self-supporting geopolymer membrane with intercepted Cr(III) for dye wastewater treatment by hybrid photocatalysis and membrane separation. *Appl Surf Sci* 515:146024.<https://doi.org/10.1016/j.apsusc.2020.146024>
 15. Chen X, Hu Y, Xie Z, Wang H (2018) *Membranes* 71–96.
 16. Chi L, Qian Y, Guo J, Wang X, Arandiyán H, Jiang Z (2019) Novel g-C₃N₄/TiO₂/PAA/PTFE ultrafiltration membrane enabling enhanced antifouling and exceptional visible-light photocatalytic self-cleaning. *Catal Today* 335:527–537. <https://doi.org/10.1016/j.cattod.2019.02.027>
 17. Chong MN, Jin B, Chow CWK, Saint C (2010) Recent developments in photocatalytic water treatment technology: a review. *Water Res* 44:2997–3027. <https://doi.org/10.1016/j.watres.2010.02.039>
 18. Cui Z (2015) Encyclopedia of membranes. *Encycl Membr*, 1–2.<https://doi.org/10.1007/978-3-642-40872-4>
 19. Damodar RA, You SJ, Ou SH (2010) Coupling of membrane separation with photocatalytic slurry reactor for advanced dye wastewater treatment. *Sep Purif Technol* 76:64–71. <https://doi.org/10.1016/j.seppur.2010.09.021>
 20. Fakirov S (2016) Nano-size polymers: preparation, properties, applications. *Nano-Size Polym Prep Prop Appl*, 1–399.<https://doi.org/10.1007/978-3-319-39715-3>

21. Figoli A, Marino T, Galiano F (2016) Polymeric membranes in biorefinery. *Membr Technol Biorefining*<https://doi.org/10.1016/B978-0-08-100451-7.00002-5>
22. Fryczkowska B (2018) The application of ultrafiltration composite GO/PAN membranes for removing dyes from textile wastewater. *Desalin Water Treat* 128:79–88. <https://doi.org/10.5004/dwt.2018.22599>
23. Ganesh BM, Isloor AM, Ismail AF (2013) Enhanced hydrophilicity and salt rejection study of graphene oxide-polysulfone mixed matrix membrane. *Desalination* 313:199–207. <https://doi.org/10.1016/j.desal.2012.11.037>
24. Gürses A, Açıkyıldız M, Güneş K, Gürses MS (2016) dyes and pigments: their structure and properties. In: *Dyes and pigments*. Springer briefs in molecular science. Springer, Cham. <https://doi.org/10.1007/978-3-319-33892-72>
25. Holkar CR, Jadhav AJ, Pinjari DV, Mahamuni NM, Pandit AB (2016) A critical review on textile wastewater treatments: Possible approaches. *J. Environ Manag* 182:351–366. <https://doi.org/10.1016/j.jenvman.2016.07.090>
26. Horovitz I, Horovitz I, Gitis V, Avisar D, Mamane H (2020) Ceramic-based photocatalytic membrane reactors for water treatment—where to next? *Rev Chem Eng* 36:593–622.<https://doi.org/10.1515/revce-2018-0036>
27. Hořda AK, Vankelecom IFJ (2015) Understanding and guiding the phase inversion process for synthesis of solvent resistant nanofiltration membranes. *J Appl Polym Sci* 132:1–17. <https://doi.org/10.1002/app.42130>
28. Hussien MSA, Mohammed MI, Yahia IS (2020) Flexible photocatalytic membrane based on CdS/PMMA polymeric nanocomposite films: multifunctional materials. *Environ Sci Pollut Res* 27:45225–45237. <https://doi.org/10.1007/s11356-020-10305-1>
29. IARC monographs on the evaluation of carcinogenic risks to humans (2010) IARC Monogr Eval Carcinog Risks to Humans 93:9–38.<https://doi.org/10.1136/jcp.48.7.691-a>
30. Iglesias O, Rivero MJ, Urtiaga AM, Ortiz I (2016) Membrane-based photocatalytic systems for process intensification. *Chem Eng J* <https://doi.org/10.1016/j.cej.2016.01.047>
31. Jose Varghese R, Sakho EHM, Parani S, Thomas S, Oluwafemi OS, Wu J (2019) Introduction to nanomaterials: synthesis and applications. *Nanomater. Sol Cell Appl* 75–95. <https://doi.org/10.1016/B978-0-12-813337-8.00003-5>
32. Kiwaan HA, Atwee TM, Azab EA, El-Bindary AA (2020) Photocatalytic degradation of organic dyes in the presence of nanostructured titanium dioxide. *J Mol Struct* 1200. <https://doi.org/10.1016/j.molstruc.2019.127115>
33. Koe WS, Lee JW, Chong WC, Pang YL, Sim LC (2020) An overview of photocatalytic degradation: photocatalysts, mechanisms, and development of photocatalytic membrane. *Environ Sci Pollut Res* 27:2522–2565. <https://doi.org/10.1007/s11356-019-07193-5>
34. Konstantinou IK, Albanis TA (2004) TiO₂-assisted photocatalytic degradation of azo dyes in aqueous solution: kinetic and mechanistic investigations: a review. *Appl Catal B Environ* 49:1–14. <https://doi.org/10.1016/j.apcatb.2003.11.010>
35. Koutahzadeh N, Esfahani MR, Arce PE (2016) Sequential use of UV/H₂O₂-(PSF/TiO₂/MWCNT) mixed matrix membranes for dye removal in water purification: membrane permeation, fouling, rejection, and decolorization. *Environ Eng Sci* 33:430–440. <https://doi.org/10.1089/ees.2016.0023>
36. Kristine N, Cruz O, Uy G, Senoro DB, You S, Lu S (2014) Journal of the Taiwan Institute of Chemical Engineers Dye degradation and antifouling properties of polyvinylidene fluoride/titanium oxide membrane prepared by sol–gel method. *J Taiwan Inst Chem Eng* 45:192–201
37. Kumari P, Bahadur N, Dumée LF (2020) Photo-catalytic membrane reactors for the remediation of persistent organic pollutants—a review. *Sep Purif Technol* 230:115878.<https://doi.org/10.1016/j.seppur.2019.115878>
38. Kuvarega AT, Khumalo N, Dlamini D, Mamba BB (2018) Polysulfone/N, Pd co-doped TiO₂ composite membranes for photocatalytic dye degradation. *Sep Purif Technol* 191:122–133. <https://doi.org/10.1016/j.seppur.2017.07.064>

39. Lavielle N, Hebraud A, Schlatter G, Lind T-M, Rossi RM, Popa A (2013) Straightforward approach for fabricating hierarchically structured composite membranes. *ACS Appl Mater Interfaces* 5:10090–10097
40. Lellis B, Fávoro-Polonio CZ, Pamphile JA, Polonio JC (2019) Effects of textile dyes on health and the environment and bioremediation potential of living organisms. *Biotechnol Res Innov* 3:275–290. <https://doi.org/10.1016/j.biori.2019.09.001>
41. Leong S, Razmjou A, Wang K, Hapgood K, Zhang X, Wang H (2014) TiO₂ based photocatalytic membranes: a review. *J Memb Sci* 472:167–184. <https://doi.org/10.1016/j.memsci.2014.08.016>
42. Mandegari M, Fashandi H (2017) Untapped potentials of acrylonitrile-butadiene-styrene/polyurethane (ABS/PU) blend membrane to purify dye wastewater. *J Environ Manage* 197:464–475. <https://doi.org/10.1016/j.jenvman.2017.04.026>
43. Mastropietro TF, Meringolo C, Poerio T, Scarpelli F, Godbert N, Di Profio G, Fontananova E (2017) Multistimuli Activation of TiO₂/α-alumina membranes for degradation of methylene blue. *Ind Eng Chem Res* 56:11049–11057. <https://doi.org/10.1021/acs.iecr.7b02778>
44. Mohamad Said KA, Ismail AF, Karim ZA, Abdullah MS, Usman J, Raji YO (2020) Innovation in membrane fabrication: Magnetic induced photocatalytic membrane. *J Taiwan Inst Chem Eng* 113:372–395. <https://doi.org/10.1016/j.jtice.2020.08.014>
45. Molinari R, Argurio P, Bellardita M, Palmisano L (2017) Photocatalytic processes in membrane reactors, comprehensive membrane science and engineering. <https://doi.org/10.1016/B978-0-12-409547-2.12220-6>
46. Mozia S (2010) Photocatalytic membrane reactors (PMRs) in water and wastewater treatment. *A Rev Sep Purif Technol* 73:71–91. <https://doi.org/10.1016/j.seppur.2010.03.021>
47. Mpelane A, Katwire DM, Mungondori HH, Nyamukamba P, Taziwa RT (2020) Application of novel c-tio2-cfa/pan photocatalytic membranes in the removal of textile dyes in wastewater. *Catalysts* 10:1–17. <https://doi.org/10.3390/catal10080909>
48. Muhd Julkapli N, Bagheri S, Bee Abd Hamid S (2014) Recent advances in heterogeneous photocatalytic decolorization of synthetic dyes. *Sci World J.* <https://doi.org/10.1155/2014/692307>
49. Norrman K, Ghanbari-Siahkali A, Larsen NB (2005) Studies of spin-coated polymer films. *Annu Reports Prog Chem Sect C* 101:174–201. <https://doi.org/10.1039/b408857n>
50. Park H, Kim HI, Moon GH, Choi W (2016) Photoinduced charge transfer processes in solar photocatalysis based on modified TiO₂. *Energy Environ Sci* 9:411–433. <https://doi.org/10.1039/c5ee02575c>
51. Penboon L, Khruetakham A, Sairiam S (2019) TiO₂ coated on PVDF membrane for dye wastewater treatment by a photocatalytic membrane. *Water Sci Technol* 79:958–966. <https://doi.org/10.2166/wst.2019.023>
52. Rajeshwar K, Osugi ME, Chanmanee W, Chenthamarakshan CR, Zaroni MVB, Kajitvichyanukul P, Krishnan-Ayer R (2008) Heterogeneous photocatalytic treatment of organic dyes in air and aqueous media. *J Photochem Photobiol C Photochem Rev* 9:171–192. <https://doi.org/10.1016/j.jphotochemrev.2008.09.001>
53. Rajeswari A, Vismaiya S, Pius A (2017) Preparation, characterization of nano ZnO-blended cellulose acetate-polyurethane membrane for photocatalytic degradation of dyes from water. *Chem Eng J. Elsevier B.V.* <https://doi.org/10.1016/j.cej.2016.10.124>
54. Rauf MA, Hisaindee S (2013) Studies on solvatochromic behavior of dyes using spectral techniques. *J Mol Struct* 1042:45–56. <https://doi.org/10.1016/j.molstruc.2013.03.050>
55. Samsami S, Mohamadi M, Sarrafzadeh MH, Rene ER, Firoozbahr M (2020) Recent advances in the treatment of dye-containing wastewater from textile industries: overview and perspectives. *Process Saf Environ Prot* 143:138–163. <https://doi.org/10.1016/j.psep.2020.05.034>
56. Sathya U, Keerthi P, Nithya M, Balasubramanian N (2020) Development of photochemical integrated submerged membrane bioreactor for textile dyeing wastewater treatment. *Environ Geochem Health* 0123456789. <https://doi.org/10.1007/s10653-020-00570-x>
57. Schneller T, Waser R, Kosec M, Payne D (2013) Chemical solution deposition of functional oxide thin films. *Chem Solut Depos Funct Oxide Thin Film* 9783211993:1–796. <https://doi.org/10.1007/978-3-211-99311-8>

58. Singh R, Sinha MK, Purkait MK (2020) Stimuli responsive mixed matrix polysulfone ultra-filtration membrane for humic acid and photocatalytic dye removal applications. *Sep Purif Technol* 250:117247. <https://doi.org/10.1016/j.seppur.2020.117247>
59. Su CXH, Low LW, Teng TT, Wong YS (2016) Combination and hybridisation of treatments in dye wastewater treatment: A review. *J Environ Chem Eng* 4:3618–3631. <https://doi.org/10.1016/j.jece.2016.07.026>
60. Subramaniam MN, Goh PS, Lau WJ, Ng BC, Ismail AF (2018) Development of nanomaterial-based photocatalytic membrane for organic pollutants removal. *Advanced nanomaterials for membrane synthesis and its applications*. Elsevier Inc. <https://doi.org/10.1016/B978-0-12-814503-6.00003-3>
61. Tang X, Yan X (2017) Dip-coating for fibrous materials: mechanism, methods and applications. *J Sol-Gel Sci Technol* 81:378–404. <https://doi.org/10.1007/s10971-016-4197-7>
62. Tijing LD, Woo YC, Yao M, Ren J, Shon HK (2017) 1.16 Electrospinning for membrane fabrication: strategies and applications. *Compr Membr Sci Eng* 1:418–444. <https://doi.org/10.1016/b978-0-12-409547-2.12262-0>
63. Viswanathan B (2017) Photocatalytic degradation of dyes: an overview. *Curr Catal* 7:99–121. <https://doi.org/10.2174/2211544707666171219161846>
64. Wang M, Yang G, Jin P, Tang H, Wang H, Chen Y (2016) Highly hydrophilic poly(vinylidene fluoride)/meso-titania hybrid mesoporous membrane for photocatalytic membrane reactor in water. *Sci Rep* 6:1–10. <https://doi.org/10.1038/srep19148>
65. Wang M, Zhang Y, Yu G, Zhao J, Chen X, Yan F, Li J, Yin Z, He B (2020) Monolayer porphyrin assembled SPSf/PES membrane reactor for degradation of dyes under visible light irradiation coupling with continuous filtration. *J Taiwan Inst Chem Eng* 109:62–70. <https://doi.org/10.1016/j.jtice.2020.02.013>
66. Wu XQ, Shen JS, Zhao F, Shao ZD, Zhong LB, Zheng YM (2018) Flexible electrospun MWCNTs/Ag₃PO₄/PAN ternary composite fiber membranes with enhanced photocatalytic activity and stability under visible-light irradiation. *J Mater Sci* 53:10147–10159. <https://doi.org/10.1007/s10853-018-2334-0>
67. Zangeneh H, Zinatizadeh AAL, Habibi M, Akia M, Hasnain Isa M (2015) Photocatalytic oxidation of organic dyes and pollutants in wastewater using different modified titanium dioxides: a comparative review. *J Ind Eng Chem* 26:1–36. <https://doi.org/10.1016/j.jiec.2014.10.043>
68. Zeng H, Yu Z, Shao L, Li X, Zhu M, Liu Y, Feng X, Zhu X (2020) Ag₂CO₃@UiO-66-NH₂ embedding graphene oxide sheets photocatalytic membrane for enhancing the removal performance of Cr(VI) and dyes based on filtration. *Desalination* 491:114558. <https://doi.org/10.1016/j.desal.2020.114558>
69. Zhang L, Mohamed HH, Dillert R, Bahnemann D (2012) Kinetics and mechanisms of charge transfer processes in photocatalytic systems: A review. *J Photochem Photobiol C Photochem Rev* 13:263–276. <https://doi.org/10.1016/j.jphotochemrev.2012.07.002>
70. Zhang X, Wang DK, Diniz Da Costa JC (2014) Recent progresses on fabrication of photocatalytic membranes for water treatment. *Catal Today* 230:47–54. <https://doi.org/10.1016/j.cattod.2013.11.019>
71. Zheng X, Shen ZP, Shi L, Cheng R, Yuan DH (2017) Photocatalytic membrane reactors (PMRs) in water treatment: configurations and influencing factors. *Catalysts* 7. <https://doi.org/10.3390/catal7080224>